IEEE Photonics Journal
An IEEE Photonics Society Publication

Open Access

Dimensional Transformations of Guided-Mode Resonant Photonic Lattices

Volume 12, Number 6, December 2020

Akari Watanabe
Junichi Inoue
Kenji Kintaka, ***Member, IEEE***
Shanwen Zhang
Shogo Ura, ***Member, IEEE***
Robert Magnusson, ***Life Fellow, IEEE***

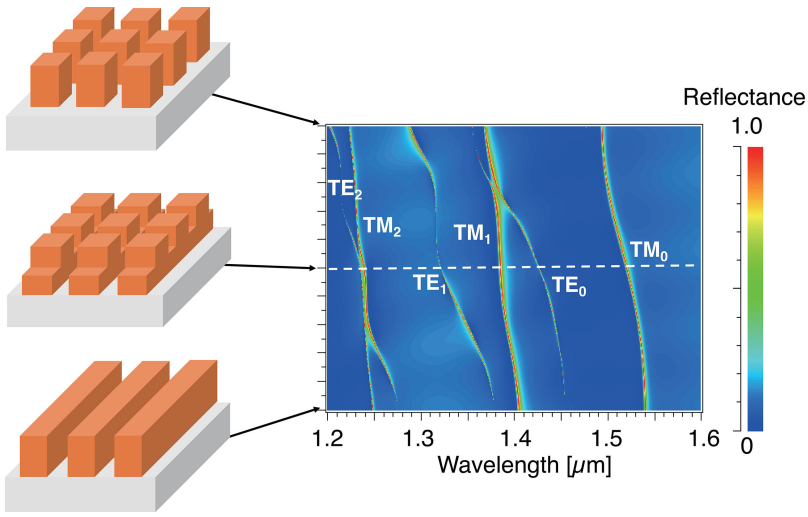

DOI: 10.1109/JPHOT.2020.3038560

IEEE photonics SOCIETY

IEEE

Dimensional Transformations of Guided-Mode Resonant Photonic Lattices

Akari Watanabe,[1] **Junichi Inoue**,[1]
Kenji Kintaka,[2] ***Member, IEEE***, **Shanwen Zhang**,[3]
Shogo Ura,[1] ***Member, IEEE***,
and Robert Magnusson,[4] ***Life Fellow, IEEE***

[1]Department of Electronics, Kyoto Institute of Technology, Kyoto 606-8585, Japan
[2]Nanomaterials Research Institute, National Institute of Advanced Industrial Science and Technology, Ikeda, Osaka 563-8577, Japan
[3]Changchun Institute of Optics, Fine Mechanics and Physics, Chinese Academy of Sciences, Changchun 130033, China
[4]Department of Electrical Engineering, University of Texas at Arlington, Arlington, Texas 76019 USA

DOI:10.1109/JPHOT.2020.3038560
This work is licensed under a Creative Commons Attribution 4.0 License. For more information, see https://creativecommons.org/licenses/by/4.0/

Manuscript received October 23, 2020; accepted November 11, 2020. Date of publication November 17, 2020; date of current version December 7, 2020. This work was supported by the National Science Foundation (NSF) under Award ECCS-1809143. Corresponding author: Akari Watanabe (e-mail: wata81624@yahoo.co.jp).

Abstract: Reflection spectra based on guided-mode resonance (GMR) are simulated and discussed with transformation between one-dimensional (1-D) and two-dimensional (2-D) photonic lattices by introducing intermediate structures consisting of vertically-stacked 1-D and 2-D gratings. Dependences of reflection spectra on a 2-D fractional ratio are investigated for two examples of narrowband and broadband resonance elements. Observed complicated spectrum transformations for the narrowband example are successfully explained by combining simple models with guided-mode indices and multilayer reflection. The understanding of the fundamental transformation dynamics will aid in the reflection band engineering for development of new optical components.

Index Terms: Subwavelength gratings, guided-mode resonance, optical filters, two-dimensional gratings, waveguides.

1. Introduction

Spatially patterned surfaces and films enable remarkable resonance effects as input light couples to leaky Bloch-type waveguide modes. When the attendant lattice has subwavelength periodicity, the observed guided-mode resonance (GMR) effects are particularly efficient with narrowband or wideband reflectance approaching unity in lossless materials [1]–[7]. It is possible to engineer device spectra for various applications in optoelectronics and photonic device technology. Thus, a GMR device may exhibit a narrowband reflection spectrum suitable for a wavelength-stabilizing external mirror of a diode laser [8]. Indeed, it is known that GMR reflectors have some advantages in design and fabrication flexibility in comparison to dielectric multilayer mirrors (DMM). For example, it is easy to control the reflection bandwidth as it is determined by coupling strength that is controlled by a guiding layer thickness, lattice depth, or fill factor. On the other hand, careful thickness and refractive-index control including material choice is required in DMM. Accordingly, various GMR filters with narrowband and broadband spectra have been reported [9], [10]. Moreover, it

is possible to design transmission-type filters as well as reflection-type devices [11] and tunable filters have also been demonstrated [5]. The basic GMR effect is polarization dependent as observed in one-dimensional (1-D) grating structures. Polarizers [12], [13], wave plates [14], [15], and de-polarizers [16], [17] have been reported. Two-dimensional (2-D) resonance elements have been widely studied on account of their polarization-independent characteristics [18], [19].

Multiple GMRs can occur when multiple guided modes are supported by a periodic waveguide. The resonance wavelengths are determined by their mode indices. It is possible to control a reflection spectrum by designing a quasi-equivalent waveguide structure. Spectral control and band engineering have been reported with 1-D and 2-D structures [20], [21]. The reflection spectrum of a 2-D GMR device is not a simple addition of two spectra of independent 1-D GMRs, but a deformed combination. There is a report to analyze the spectrum of 2-D structures by 1-D models applying effective-medium theory (EMT) [22]. However, dimensional transformations between 1-D and 2-D structures have not been reported. Characterization of intermediate structures will widen possibilities in band engineering to develop new optical components.

In this paper, we treat dimensional transformations of resonant photonic lattices by introducing intermediate structures without any EMT simplifications. It is expected that resonant guided modes will be directly identified and their transformations can be clearly seen for narrowband GMRs. In contrast, while broadband GMR filters are also attractive for various applications, guided-mode identification is not as straightforward as in the case of narrowband filters. Comparing the resonance dynamics of these limiting cases is of interest. Hence, we investigate representative resonance elements exhibiting narrowband and broadband behavior. The coupling strength determining the bandwidth depends on a refractive index modulation ${n_H}^2 - {n_L}^2$ where n_H and n_L are high and low refractive indices of the lattice, respectively. We associate our results with common materials by choosing n_H of 2.0 assuming Si_3N_4 and 3.5 assuming Si for weak and strong coupling cases, respectively, while we hold n_L at 1.0 representing operation in air environment. We emphasize that in this first study of the dimensional transformations of resonant photonic lattices, we are interested in the key resonance properties and in the details of the physical behavior as opposed to aiming for particular applications.

2. Basic Configuration and Analysis Model

In our model, a free-space wave is injected from the air into the photonic lattice vertically. The incident wave is coupled to a guided wave mode propagating along a reciprocal lattice vector, namely a grating vector in resonance condition. The quasi-guided wave is coupled again to air- and substrate-radiation waves. The substrate-radiation wave interferes with a direct transmission wave to cancel it out. Thereby, high reflectance is obtained in the resonance condition. An incident wave off resonance transmits the structure and thus the structure serves as an optical notch filter. The resonance wavelength λ_R is given by

$$\lambda_R = \Lambda N \tag{1}$$

where Λ and N denote a grating period and a guided-mode index, respectively.

A schematic view of a 1-D photonic lattice is illustrated in Fig. 1(a). A grating vector is directed along the *y*-axis and the structure is uniform in the *x*-axis direction. A schematic view of a 2-D photonic lattice is illustrated in Fig. 1(b). The grating vectors are defined along the *x*- and *y*-axes. A schematic view of an intermediate structure is illustrated in Fig. 1(c). A 2-D grating is stacked on a 1-D grating. High and low refractive indices of the gratings are denoted by n_H and n_L, respectively, while that of a substrate is n_s. Grating thicknesses of 1-D and 2-D gratings are denoted by d_{g1} and d_{g2}, respectively. The total thickness d_g is given by $d_{g1} + d_{g2}$. A grating period and a fill factor are denoted by Λ_i and F_i, respectively, where subscript $i = x$ or y represents directions along *x*- or *y*-axis. The materials are treated as being nondispersive which is a good assumption for the media and wavelength bands studied. Moreover, the media are taken to be lossless; the effect of loss is to reduce resonance efficiency and to broaden resonance linewidths that would be most evident in case of narrowband devices.

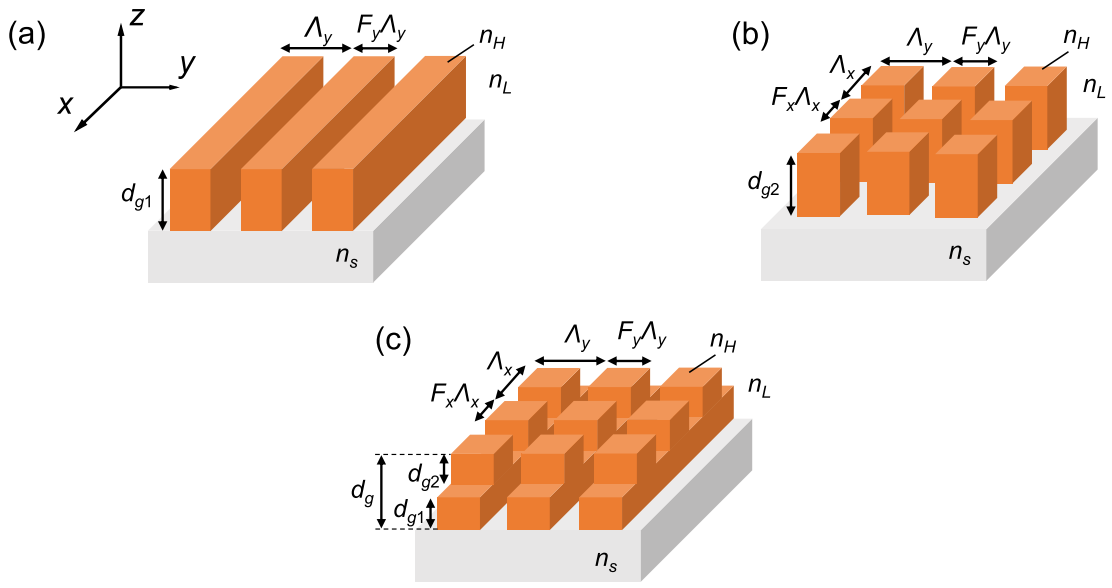

Fig. 1. Schematic views of (a) 1-D photonics lattice, (b) 2-D photonic lattice, and (c) intermediate structure.

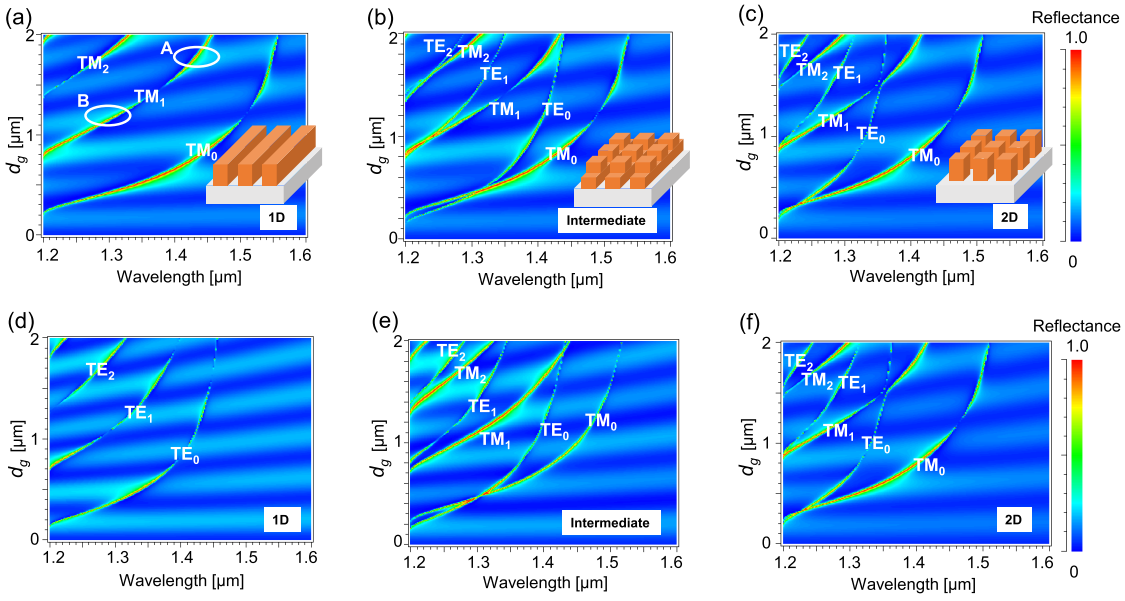

Fig. 2. Reflection spectra calculated by RCWA with *y*-polarization incidence for weakly modulated (a) 1-D lattice, (b) intermediate structure, and (c) 2-D lattice. Spectra with *x*-polarization incidence for (d) 1-D lattice, (e) intermediate structure, and (f) 2-D lattice.

3. Weakly Modulated Structure

First, we investigate reflection spectra when the modulation strength of our lattices is weak. Fig. 2 summarizes calculated reflection spectra as a function of d_g with $n_H = 2.0$, $n_L = 1.0$, $n_s = 1.5$, $\Lambda_x = \Lambda_y = 800$ nm, and $F_x = F_y = 0.9$. They are calculated by the rigorous coupled-wave analysis

(RCWA) method [23,24]. Fig. 2(a)–(c) show spectra for *y*-polarization incidence. Fig. 2(a) is a case of 1-D lattice with $d_{g1} = d_g$ and $d_{g2} = 0$. Reflectance is indicated by color. We can see narrow lines of high reflectance indicated by yellow-red color. This high reflectance is caused by GMR with transverse magnetic (TM) modes since the polarization direction and the grating vector are parallel. The reflection band is narrow, as expected from the weakly modulated structure. Interference fringes of low reflection indicated by light-blue color are also seen with low wavelength dependence. These show an interference effect of a multilayer structure. We find two extremely asymmetric shapes in the GMR reflection spectrum as shown at $d_g = 1.8$ μm ([A] in Fig. 2(a)) and 1.2 μm ([B] in Fig. 2(a)) for TM_1 mode. Spectra at [A] and [B] show steep drops at shorter and longer wavelength sides, respectively. GMR reflection spectra associated with a guided mode alternate between those two shapes as d_g increases, resulting from a phase variation of the multilayer reflection against the GMR air radiation.

Fig. 2(c) shows a case of 2-D lattice with $d_{g2} = d_g$. We can see several high-reflectance lines originating from GMR of transverse electric (TE) modes besides TM modes since one of grating vectors is orthogonal to *y*-polarization. Fig. 2(b) shows a case of an intermediate structure with $d_{g1} = d_{g2} = d_g/2$. Reflection characteristics are closer to Fig. 2(c) than Fig. 2(a) because of the inclusion of the 2-D structure. We can see redshifts in resonance wavelengths for all of the TM and TE modes as d_g increases. Fig. 2(d)–(f) show spectra for *x*-polarization incidence. Narrow lines of high reflectance result from GMR of TE modes in the case of Fig. 2(d) since the grating vector is orthogonal to the polarization. Fig. 2(f) is the same as Fig. 2(c) as it should be because of symmetry. Reflection spectra are different between *y*- and *x*-polarization in the intermediate structure as shown in Fig. 2(b) and (e).

Fig. 3 shows spectral transformations from 1-D to 2-D lattices with color-coded reflectance. The total thickness d_g is fixed to 1.6 μm. The spectra at $d_{g2}/d_g = 0$ in Fig. 3(a) and (b) are also given by the spectra at $d_g = 1.6$ μm in Fig. 2(a) and (d), respectively. The spectra at $d_{g2}/d_g = 1$ in Fig. 3(a) and (b) are the same and are also given by the spectrum at $d_g = 1.6$ μm in Fig. 2(c) or (f). We can see blueshifts in the resonance wavelength n_H for both of the TE and TM modes as d_{g2}/d_g increases. Weak undulations are seen on the blueshifted spectral loci. The resonance wavelength λ_R is determined by the mode index *N* as given in (1). The above-mentioned blueshift of λ_R, namely reduction of *N*, is caused by fractional loss of the n_H material according to the d_{g2}/d_g increase. We calculated *N* for various d_{g2}/d_g and estimated λ_R. We assumed a multilayer structure, replacing the grating by a dielectric-constant-averaged layer for the *N* calculation. The estimated λ_R for *y*-polarization incidence with TE_0 and TE_1 modes are summarized in Fig. 4(a) and (b), respectively. The dependences show good agreement with narrow lines of high reflectance shown in Fig. 3(a).

TE-mode bandwidths vary against d_{g2}/d_g, unlike that for TM modes in Fig. 3(a). The larger variation results from the higher dependence of coupling strength on d_{g2}/d_g. The increase of d_{g2}/d_g implies the growth of the grating along the *x*-direction and changes its coupling strengths of the *x*-propagating TE modes. On the other hand, TM-mode bandwidths vary unlike TE modes in Fig. 3(b). In this case, the increase of d_{g2}/d_g changes the coupling strengths of the *x*-propagating TM modes. We can see the alternation of the spectral asymmetric shape in TE modes but not in TM modes in Fig. 3(a) for d_{g2}/d_g increase, indicating a formation of a grating structure along the *x*-direction. This is consistent with the above discussion of the bandwidth variation. Moreover, Fig. 3 shows gaps in cross points of modes. In the case of *y*-polarization incidence shown in Fig. 3(a), we can see a cross at $\lambda = 1.38$ μm and $d_{g2}/d_g = 0.77$. However, they are not degenerated at the cross, indicating mode-coupling between them. The similar gap appears for *x*-polarization incidence shown in Fig. 3(b). There is a cross point at $\lambda = 1.38$ μm and $d_{g2}/d_g = 0.80$. We remark that our numerical results are fully converged as verified by comparing with cases with a larger number of spectral orders in the simulations.

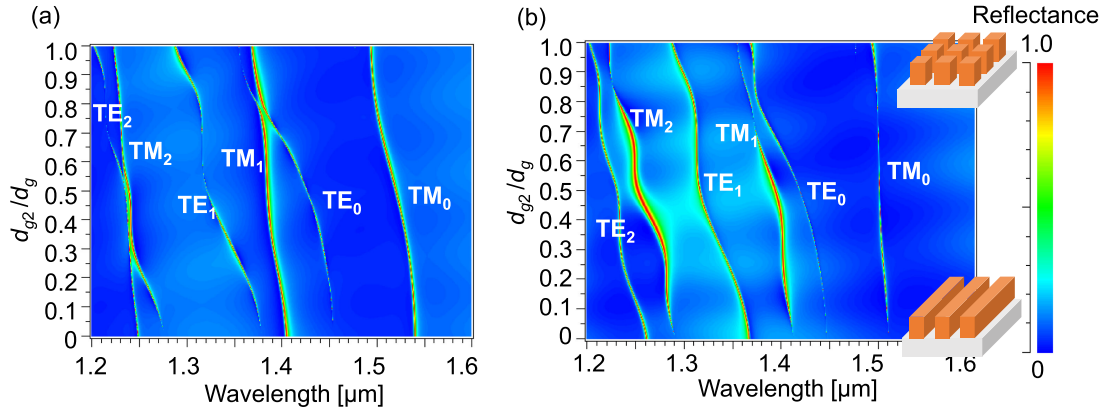

Fig. 3. Reflection spectra for weakly modulated lattices as a function of dg2/dg with (a) y- and (b) x-polarization incidence, where dg is fixed to 1.6 μm.

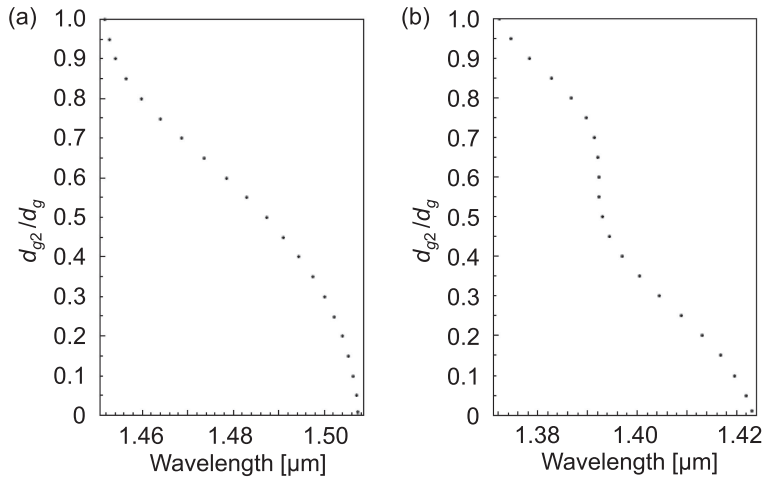

Fig. 4. The resonance wavelength λR calculated from (1) for (a) TE0 and (b) TE1 modes with y-polarization incidence.

4. Strongly Modulated Structure

In this section, we investigate the transformational dynamics of the reflection spectra under strong modulation. Fig. 5 summarizes reflection spectra as functions of d_g. The spectra are calculated for $n_H = 3.5$, $n_L = 1.0$, $n_s = 1.5$, $\Lambda_x = \Lambda_y = 630$ nm, and $F_x = F_y = 0.69$. Figs. 5(a)–(c) show spectra for *y*-polarization incidence. Fig. 5(a) is a case of 1-D lattice with $d_{g1} = d_g$ and $d_{g2} = 0$. High reflectance is obtained by GMR with TM modes. A reflection band of each guided mode is wider than the case of a weakly modulated structure as shown in Fig. 2. We can see a merger of multiple bands. Fig. 5(b) and (c) show cases of an intermediate structure with $d_{g1} = d_{g2} = d_g/2$ and 2-D lattice with $d_{g2} = d_g$, respectively. GMR lines related to TE modes appear. Reflectance decreases in some parts where GMRs of TE and TM modes occur simultaneously and interfere. In other words, high reflectance is not expected because of destructive interference of GMRs except for the case that substrate-radiation waves from both modes are in-phase to cancel the direct transmission wave. Fig. 5(d)–(f) show spectra of 1-D lattice, the intermediate structure, and 2-D lattice, respectively, for *x*-polarization incidence. Similar characteristics of merger and decrease in reflectance are seen, though reflection bands are narrower than the case of TM modes shown in Fig. 5(a) and (b).

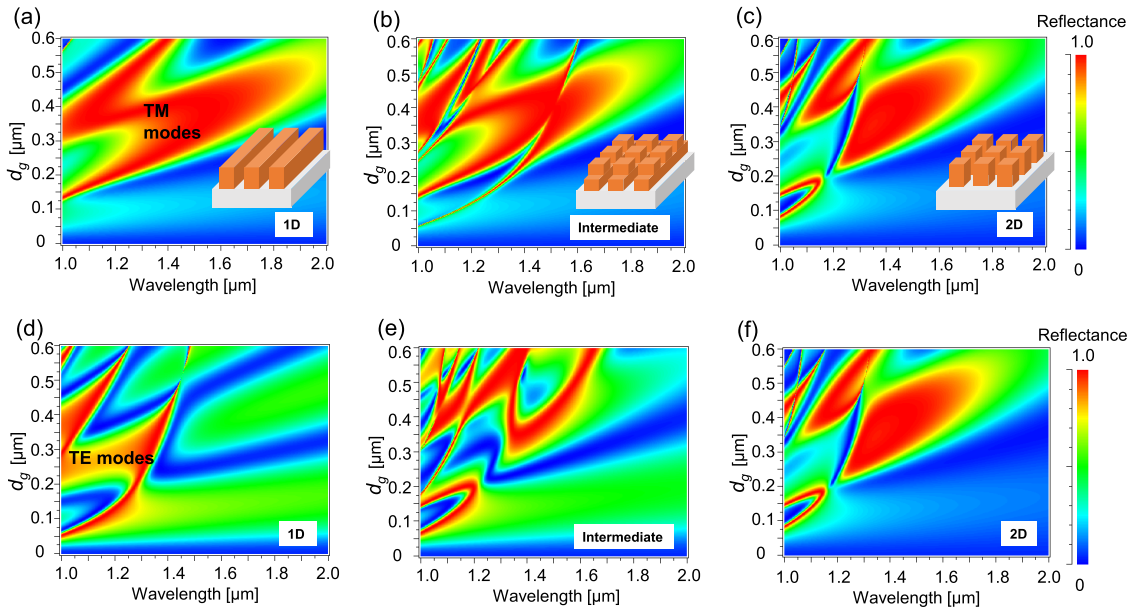

Fig. 5. Reflection spectra calculated by RCWA with *y*-polarization incidence for strongly modulated (a) 1-D lattice, (b) intermediate structure, and (c) 2-D lattice. Reflection spectra with *x*-polarization incidence for (d) 1-D lattice, (e) intermediate structure, and (f) 2-D lattice.

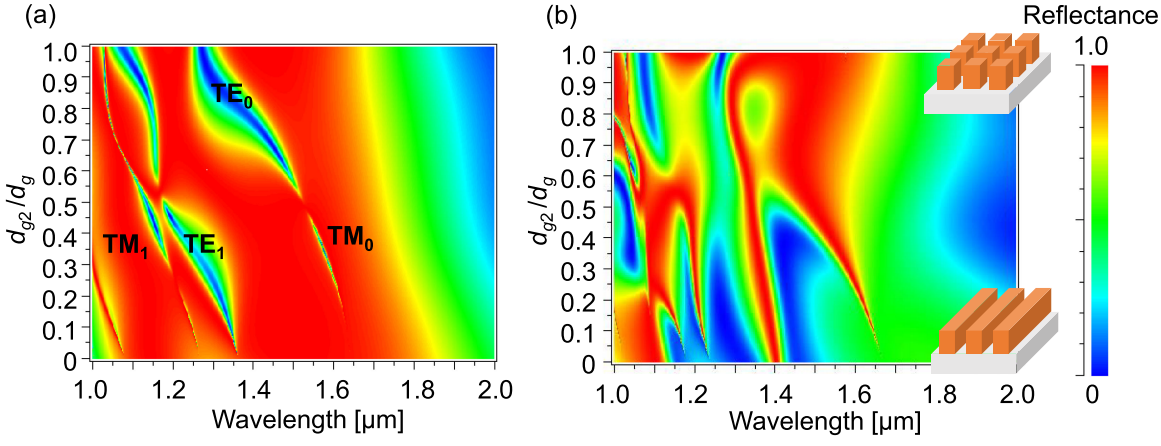

Fig. 6. Reflection spectra for strongly modulated resonant lattices as a function of d_{g2}/d_g with (a) *y*- and (b) *x*-polarization incidence, where d_g is fixed to 0.42 μm.

For strongly modulated lattices, Fig. 6 shows example spectral dynamics under dimensional transformation from 1-D to 2-D lattice with color-coded reflectance. The thickness d_g is fixed to be 0.42 μm. The spectra at $d_{g2}/d_g = 0$ in Fig. 6(a) and (b) are also given by the spectra at $d_g = 0.42$ μm in Fig. 5(a) and (d), respectively. The spectra at $d_{g2}/d_g = 1$ in Fig. 6(a) and (b) are the same and are also given by the spectrum at $d_g = 0.42$ μm in Fig. 5(c) or (f). Reflection bands associated with TM modes are wider and more stable against d_{g2}/d_g in comparison to TE-mode bands. TE modes show undulations with blueshifts as d_{g2}/d_g increases. In the case of *y*-polarization incidence shown in Fig. 6(a), GMR by TM modes is dominant and spectral variation is not so large. In the case of *x*-polarization shown in Fig. 6(b), we can see large variation in bandwidth since GMR by TE modes is dominant.

Elaborating further, it is interesting to see that simultaneous band-pass and band-stop filtering occurs in the same wavelength range for different polarizations. Band-pass filtering is obtained at $\lambda = 1.6$ μm in a range of $\lambda = 1.45 - 1.7$ μm at $d_{g2}/d_g = 0.3$ for *y*-polarization incidence as shown in Fig. 6(a), while band-stop filtering is observed for *x*-polarization incidence in Fig. 6(b). This is an example of band-engineering potential of the intermediate structure since the 1-D lattice gives spectral lines of only TE or TM modes and the full 2-D lattice delivers polarization independence.

5. Conclusion

With the aim of uncovering key properties and mechanisms, we have investigated resonant reflection spectra under dimensional transformations between 1-D and 2-D lattices. Choosing two commonly-applied materials, we map the reflectance spectra as the lattice gradually converts from a pure 1-D state to a full 2-D state. These maps display clearly key features and differences between the pure and mixed states. By tuning the 2-D fractional ratio d_{g2}/d_g in both of our narrowband and broadband examples, a diversity of spectra are brought out. Interpretation of the observed spectral transformations for the narrowband lattice example is straightforward as the resonant features are clearly seen and associated with well-defined resonance wavelengths on waveguide-mode type loci. We successfully explain them by combining simple models with guided-mode indices and multilayer reflection. The spectral dynamics under analogous transforms in heavily modulated lattices are more complex. In that case, simple models do not suffice for transparent interpretation and thus rigorous numerical modeling is essential for quantification of the spectral efficiencies and bandwidths. The understanding of these types of transformations will benefit the field of spectral band engineering for the development of new optical components. For example, we observe transition between band-pass and band-stop filtering properties on variation of the input-wave polarization state for some intermediate structures. Whereas the study provided here is theoretical only, we note that all structures presented can be expeditiously fabricated. Using UV-laser based holographic interference lithography, the full 1-D and 2-D devices are easily made; the 2-D device by applying 90° rotation between exposures. The intermediate 1-D/2-D devices are similarly fabricated but under additional exposure control.

References

[1] L. Mashev and E. Popov, "Zero order anomaly of dielectric coated gratings," *Opt. Comm.*, vol. 55, no. 6, pp. 377–380, 1985.
[2] G. A. Golubenko, A. S. Svakhin, V. A. Sychugov, and A. V. Tishchenko, "Total reflection of light from a corrugated surface of a dielectric waveguide," *Sov. J. Quantum Electron.*, vol. 15, no. 7, pp. 886–887, 1985.
[3] E. Popov, L. Mashev, and D. Maystre, "Theoretical study of the anomalies of coated dielectric gratings," *Optica Acta Int. J. Opt.*, vol. 33, no. 5, pp. 607–619, 1986.
[4] S. S. Wang, M. G. Moharam, R. Magnusson, and J. S. Bagby, "Guided-mode resonances in planar dielectric-layer diffraction gratings," *J. Opt. Soc. Am. A*, vol. 7, no. 8, pp. 1470–1474, 1990.
[5] S. S. Wang and R. Magnusson, "Theory and applications of guided-mode resonance filters," *Appl. Opt.*, vol. 32, no. 14, pp. 2606–2613, 1993.
[6] D. Rosenblatt, A. Sharon, and A. A. Friesem, "Resonant grating waveguide structures," *IEEE J. Quantum Electron.*, vol. 33, no. 11, pp. 2038–2059, Nov. 1997.
[7] P. Lalanne, J.P. Hugonin, and P. Chavel, "Optical properties of deep lamellar Gratings: A coupled Bloch-mode insight," *J. Lightw. Technol.*, vol. 24, no. 6, pp. 2442–2449, 2006.
[8] I. Avrutsky and R. Rabady, "Waveguide grating mirror for large-area semiconductor lasers," *Opt. Lett.*, vol. 26, no. 13, pp. 989–991, 2001.
[9] D. L. Brundrett, E. N. Glytsis, and T. K. Gaylord, "Normal-incidence guided-mode resonant grating filters: Design and experimental demonstration," *Opt. Lett.*, vol. 23, no. 9, pp. 700–702, 1998.
[10] T. Khaleque, M. J. Uddin, and R. Magnusson, "Design and fabrication of broadband guided-mode resonant reflectors in TE polarization," *Opt. Exp.*, vol. 22, no. 10, pp. 12349–12358, 2014.
[11] Y. Ding and R. Magnusson, "Doubly resonant single-layer bandpass optical filters," *Opt. Lett.*, vol. 29, no. 10, pp. 1135–1137, 2004.
[12] K. J. Lee *et al.*, "Silicon-layer guided-mode resonance polarizer with 40-nm bandwidth," *IEEE Photon. Technol. Lett.*, vol. 20, no. 22, pp. 1857–1859, Nov., 2008.
[13] A. Arbabi, Y. Horie, M. Bagheri, and A. Faraon, "Dielectric metasurfaces for complete control of phase and polarization with subwavelength spatial resolution and high transmission," *Nat. Nanotechnol.*, vol. 10, no. 11, pp. 937–943, 2015.

[14] R. Magnusson, M. Shokooh-Saremi, and E. G. Johnson, "Guided-mode resonant wave plates," *Opt. Lett.*, vol. 35, no. 14, pp. 2472–2474, 2010.
[15] D. C. Flanders, "Submicrometer periodicity gratings as artificial anisotropic dielectrics," *Appl. Phys. Lett.*, vol. 42, no. 6, pp. 492–494, 1983.
[16] G. Biener, A. Niv, V. Kleiner, and E. Hasman, "Computer-generated infrared depolarizer using space-variant subwavelength dielectric gratings," *Opt. Lett.*, vol. 28, no. 16, pp. 1400–1402, 2003.
[17] I. Vartiainen, J. Tervo, and M. Kuittinen, "Depolarization of quasi-monochromatic light by thin resonant gratings," *Opt. Lett.*, vol. 34, no. 11, pp. 1648–1650, 2009.
[18] S. Peng and G. M. Morris, "Resonant scattering from two-dimensional gratings," *J. Opt. Soc. Am. A*, vol. 13, no. 5, pp. 993–1005, 1996.
[19] D. W. Peters *et al.*, "Demonstration of polarization-independent resonant subwavelength grating filter arrays," *Opt. Lett.*, vol. 35, no. 19, pp. 3201–3203, 2010.
[20] E. Popov, A.-L. Fehrembach, Y. Brûlé, G. Demésy, and P. Boyer, "Two-dimensional grating for narrow-band filtering with large angular tolerances," *Opt. Exp.*, vol. 24, no. 13, pp. 14974–14985, 2016.
[21] M. Shokooh-Saremi and R. Magnusson, "Properties of two-dimensional resonant reflectors with zero-contrast gratings," *Opt. Lett.*, vol. 39, no. 24, pp. 6958–6961, 2014.
[22] Y. H. Ko, M. Shokooh-Saremi, and R. Magnusson, "Modal processes in two-dimensional resonant reflectors and their correlation with spectra of one-dimensional equivalents," *IEEE Photon. J.*, vol. 7, no. 5, Oct. 2015, Art. no. 4900210.
[23] T. K. Gaylord and M. G. Moharam, "Analysis and applications of optical diffraction by gratings," *Proc. IEEE*, vol. 73, no. 5, pp. 894–937, May 1985.
[24] M. G. Moharam, "Coupled-wave analysis of two-dimensional dielectric gratings," *Proc. SPIE*, vol. 883, 1988, pp. 8–11.